High-throughput screen identifies MAS9 as a novel inhibitor of the C-type lectin receptor-2 (CLEC-2)–podoplanin interaction

Received: 20 May 2024 | Revised: 21 November 2024 | Accepted: 2 March 2025

DOI: 10.1111/bph.70036

RESEARCH ARTICLE

High-throughput screen identifies MAS9 as a novel inhibitor of the C-type lectin receptor-2 (CLEC-2)–podoplanin interaction

Marcin A. Sowa[1,2,3] | Yan Wu[1] | Jan van Groningen[4] | Ying Di[5] | Helma van den Hurk[4] | Johannes A. Eble[6] | Jonathan M. Gibbins[1] | Ángel García[2,3] | Alice Y. Pollitt[1]

[1]Institute for Cardiovascular and Metabolic Research (ICMR), School of Biological Sciences, University of Reading, Reading, UK

[2]Platelet Proteomics Group, Center for Research in Molecular Medicine and Chronic Diseases (CiMUS), Universidade de Santiago de Compostela, Santiago de Compostela, Spain

[3]Instituto de Investigación Sanitaria de Santiago (IDIS), Santiago de Compostela, Spain

[4]Pivot Park Screening Centre, Oss, The Netherlands

[5]Institute of Cardiovascular Sciences, College of Medical and Dental Sciences, University of Birmingham, Birmingham, UK

[6]Institute for Physiological Chemistry and Pathobiochemistry, University of Münster, Münster, Germany

Correspondence
Alice Y. Pollitt, Institute for Cardiovascular and Metabolic Research (ICMR), School of Biological Sciences, University of Reading, Reading, UK.
Email: a.pollitt@reading.ac.uk

Funding information
Spanish Ministry of Science, Innovation and Universities, Grant/Award Numbers: PDC2022-133743-I00, PID2019-108727RB-I00; H2020 Marie Skłodowska-Curie Actions, Grant/Award Number: 766118; Academy of Medical Sciences, Grant/Award Number: SBF002\1099; Deutsche Forschungsgemeinschaft, Grant/Award Number: Eb177/19-1 (project number: 414847370); National Centre for the Replacement Refinement and Reduction of Animals in Research, Grant/Award Number: NC/Y000870/1

Abstract

Background and Purpose: The C-type lectin-like receptor-2 (CLEC-2) is a platelet receptor for the endogenous ligand podoplanin. This interaction contributes to several (patho)physiological processes, such as lymphangiogenesis, preservation of blood and lymphatic vessel integrity organ development, and tumour metastasis. Activation of CLEC-2 leads to the phosphorylation of its cytoplasmic hemITAM domain and initiates a signalling cascade involving the kinase Syk. The aim of this study was to identify and characterise a novel small molecule inhibitor of CLEC-2.

Experimental Approach: An AlphaScreen-based high-throughput screening was used to identify a small molecule inhibitor of the CLEC-2–podoplanin interaction. Binding site interactions were assessed using in silico modelling. Functional assays, including light transmission aggregometry, platelet spreading and phosphorylation assays, were used to evaluate the effect of a small molecule on CLEC-2-mediated platelet activation.

Key Results: A total of 18,476 small molecules were screened resulting in 14 candidates. Following secondary screening, one novel small molecule, MAS9, was taken forward for further characterisation. The binding sites of MAS9 to CLEC-2 were predicted to share binding sites with the CLEC-2 ligands podoplanin and rhodocytin. MAS9 inhibited CLEC-2-mediated platelet aggregation, spreading and signalling. MAS9 also resulted in inhibited fibrinogen binding.

Conclusion and Implications: MAS9 inhibits CLEC-2-mediated aggregation, platelet spreading and signalling, showing selectivity of CLEC-2 inhibition over GPVI. This study paves the way for future preclinical assays to test the potential of MAS9 as a novel therapeutic tool to treat pathologies such as thromboinflammation and cancer.

KEYWORDS
AlphaScreen, CLEC-2, platelet, podoplanin, small molecule

Abbreviations: CLEC-2, C-type lectin-like receptor 2; CRP-XL, cross-linked collagen-related peptide; GPVI, glycoprotein VI; HDLECs, human dermal lymphatic endothelial cells; MAS9, ethyl 1-[(8-hydroxy-5-quinolinyl)methyl]-3-piperidinecarboxylate.

1 | INTRODUCTION

A promising avenue in the development of therapeutics is the targeted disruption of specific protein–protein interactions that are pivotal in disease pathogenesis. The C-type lectin-like receptor-2 (CLEC-2) and its ligand, podoplanin, represent one such interaction of therapeutic potential and plays a significant role in a variety of pathophysiological processes, including tumour metastasis, lymphatic vessel formation and thrombo-inflammation (Haining et al., 2021; Meng et al., 2021; Suzuki-Inoue, 2019). Other ligands are emerging to increase CLEC-2's potential as a drug target. For example, hemin, a product of haemolysis released during red blood cell destruction, has been identified as a novel endogenous activatory ligand for CLEC-2 (Bourne et al., 2021).

Ligand binding to CLEC-2 triggers the phosphorylation of a tyrosine residue in its cytoplasmic hemITAM domain by **Src** and **Syk** (Fuller et al., 2007; Spalton et al., 2009), leading to activation of these kinases and initiating the assembly of the "LAT signalosome" resulting in **phospholipase C gamma 2** (PLCγ2) activation (Izquierdo et al., 2020; Severin et al., 2011). PLCγ2 induces hydrolysis of **phosphatidylinositol 4,5-bisphosphate** (PIP_2), leading to formation of the second messengers diacylglycerol (DAG) and **inositol trisphosphate** (IP_3) (Berridge et al., 2003). It stimulates **protein kinase C** (PKC) and the release of Ca^{2+}. This signalling pathway results in the secretion of dense and α-granules and "inside-out" signalling activation of **integrin $\alpha_{IIb}\beta_3$**, leading to platelet aggregation (Ma et al., 2007).

There are only three known small molecule inhibitors of the CLEC–podoplanin interaction. The first, cobalt-hematoporphyrin, blocks tumour metastasis and thrombosis in mice (Tsukiji et al., 2018). However, because of its low potency, toxicity and lack of oral availability, it cannot be pursued for clinical development (Tsukiji et al., 2018). The second, 2CP, also blocked tumour metastasis and thrombosis in mice and inhibits tumour cell-induced platelet aggregation (Chang et al., 2015). Although 2CP inhibited podoplanin-induced aggregation, 2CP had no inhibitory effect on snake venom, rhodocytin-induced, platelet aggregation. These data indicate that 2CP may have a low affinity for CLEC-2 by failing to displace rhodocytin. Alternatively, this difference may be a result of distinct binding properties of podoplanin and rhodocytin for CLEC-2 when compared with 2CP (Chang et al., 2015; Watson et al., 2007). Diphenyl-tetrazol-propanamide derivatives have recently been identified as small molecules that can inhibit CLEC-2. However, these derivatives are not limited to CLEC-2 and also inhibit glycoprotein VI (GPVI) (Watanabe et al., 2024).

Antibodies targeting human CLEC-2, such as AYP1, can block the CLEC-2–podoplanin interaction (Gitz et al., 2014). Nevertheless, most antibodies that block the interaction between human CLEC-2 and podoplanin have been developed against podoplanin. On the other hand, small molecule inhibitors offer several advantages over antibodies as potential therapies; for example, they can be delivered orally rather than by invasive routes and have the potential to be economically sustainable. There is a need to develop CLEC-2 inhibitors that overcome the limitations, in terms of potency, toxicity or specificity exhibited by previously identified small molecule inhibitors. We sought to identify novel small molecule inhibitors for the CLEC-2–podoplanin interaction by developing an AlphaScreen assay to screen 18,476 compounds. We characterised the identified one small molecule using a range of functional tests and explored its interaction with CLEC-2 using in silico modelling.

What is already known

- The CLEC-2–podoplanin interaction is a promising target for development of antiplatelet drugs against thrombo-inflammation.
- Existing small molecule inhibitors exhibit limitations in terms of potency, toxicity or specificity.

What does this study add

- MAS9 was identified as a novel small molecule inhibitor targeting the CLEC-2–podoplanin interaction.
- MAS9 inhibited CLEC-2-mediated platelet aggregation, adhesion and signalling.

What is the clinical significance

- MAS9 is a promising compound targeting CLEC-2, with potential therapeutic application.
- Selective inhibition of CLEC-2-mediated processes provides a targeted approach with potential clinical benefits.

2 | METHODS

2.1 | Materials

Recombinant human Podoplanin-rFc (Morán et al., 2022), recombinant human histidine-tagged CLEC-2/CLEC1B (Cat# 1718-CL; R&D systems, RRID:SCR_006140), 1536-well microplates (3725, Corning), cross-linked collagen-related peptide (CRP-XL; Cambcol), rhodocytin purified from the venom of *Calloselasma rhodostoma* as previously described (Eble et al., 2001), Alexa Fluor 488-conjugated **fibrinogen** (Invitrogen Cat# F13191), PE/Cy5 conjugated anti-human **P-selectin** (AK-4; BD Biosciences, Cat# 551142, RRID:AB_394070), PE-Cy™5 Mouse IgG1 κ Isotype Control (MOPC-21, BD Biosciences, Cat# 555750, RRID:AB_396092), APC conjugated anti-human CD42b (HIP1; BD Biosciences, Cat# 551061, RRID:AB_398486), anti-podoplanin (Insight Biotechnology Cat# 11-009, RRID:AB_3676761) Anti-phospho tyrosine antibody (4G10, Millipore Cat# 05-321X, RRID:AB_568858), anti-phospho Syk 525/526 antibody (Abcam

Cat# ab58575, RRID:AB_882780), anti-Syk antibody (Santa Cruz Biotechnology Cat# sc-1240, RRID:AB_628308) and anti-GAPDH antibody (Abcam Cat# ab201822, RRID:AB_2927782). Goat anti-Rabbit IgG (H + L) Secondary Antibody, HRP (Invitrogen, Cat# 31460, RRID:AB_228341), Goat anti-Mouse IgG (H + L) Secondary Antibody, HRP (Invitrogen, Cat# 31430, RRID:AB_228307), Alexa Fluor 647 conjugated Phalloidin (Invitrogen, Cat# A22287). **Thrombin**, **indomethacin**, **apyrase** (Merck), **U46619** (Enzo), **eptifibatide** (Integrilin; GlaxoSmithKline), Hydromount (National Diagnostics #HS-106) and MAS9 (AP-906/41650495, SPECS, www.specs.net).

2.2 | Preparation of MAS9

MAS9 was reconstituted in DMSO at 10 mM. MAS9 was then further diluted in phosphate buffered saline (PBS) on the experimental day. The final concentration of DMSO in the platelet assays was maintained at 0.3% (v/v). Following preincubation of the indicated final concentrations of MAS9 for the indicated time, MAS9 was not removed from the experimental assays.

2.3 | High Throughput Screening (HTS)

HTS was performed using the Pivot Park Screening Centre library (18,476 compounds composed of the Prestwick Chemical and SPECS libraries) and carried out using an Amplified Luminescent Proximity Homogeneous Assay (AlphaScreen™, Perkin-Elmer). The assay was performed using biotinylated recombinant human Podoplanin-rFc, coupled to donor beads and recombinant human histidine-tagged CLEC-2, coupled to acceptor beads.

Firstly, 10 nl of 18,476, 2-mM compounds, dissolved in 100% DMSO, were dispensed into 1536-well microplates using an Echo® 555 acoustic liquid dispenser; 100% DMSO was used as a control. Secondly, 0.5 µl of reaction buffer (0.1% BSA in PBS) was added to wells using a Certus Flex liquid dispenser; 0.5 µl of 160 µM of cobalt hematoporphorin, a known inhibitor of the CLEC-2–podoplanin interaction, was used as a positive control (Tsukiji et al., 2018). Biotinylated recombinant human podoplanin-rFc, and recombinant human HIS-tagged CLEC-2 were diluted into reaction buffer to 100 and 400 nM, respectively, and added at a 1:1 ratio to all wells, reaction buffer was used as a control. Following a 30-min incubation at room temperature, 25 $\mu g \cdot ml^{-1}$ of nickel-chelate acceptor beads were added to all wells for 1 h at room temperature in the dark, followed by a further 1-h incubation with 25 $\mu g \cdot ml^{-1}$ of streptavidin donor beads. The fluorescence intensity at 520/620 nm (ex/em) was subsequently read using an Envision multi-label plate reader (Perkin-Elmer). The signal-to-background (S/B) ratio was calculated by dividing the mean of the maximum fluorescent signal by the mean of the minimum fluorescent signal to determine the fluorescence change in the assay. An AlphaScreen TruHits kit® was used to identify false positive results from the primary screen (Perkin-Elmer).

2.4 | Protein-ligand in silico modelling

For in silico molecular docking of MAS9 to CLEC-2, the human CLEC-2 structure (PDB: 2C6U) was used. The protein structure was prepared and optimised using the Protein Preparation Wizard in Maestro Schrödinger (Release 2020-4) during which missing hydrogens were added, the ionisation states at pH 7.0 ± 2.0 were generated by Epik, and water molecules were removed beyond 5 Å from nonstandard residues. H-bond assignment was optimised using PROPK-A (pH 7.0) and the structure minimised using an OPLS4 (Optimised Potentials of Liquid Simulations) force field. MAS9 has one chiral centre at the 3-position of the piperidine ring. With one chiral centre, there are two stereoisomers, corresponding to the R and S configurations at that chiral centre (Figure S1). Both stereoisomers were docked. The 3D structures of MAS9 were generated using the Ligprep module in Maestro Schrödinger and minimised using OPLS4. MAS9 was docked using the GLIDE (Grid-based Ligand Docking with Energetic) module in Maestro Schrödinger using the standard precision mode by enabling flexible ligand sampling during docking.

The grid was centralised around the CLEC-2–podoplanin and rhodocytin binding sites (Arg107, Arg118, Arg152, Arg157) with a side length of 5 Å. Confirmations were ranked based on their GLIDE docking scores. The grid was centralised around the known common binding sites thought to induce CLEC-2 activation by podoplanin and rhodocytin and was based on their crystal structures (PDB: 3WSR for podoplanin and 3WWK for rhodocytin). There are four arginine residues: Arg107, Arg118, Arg152 and Arg157. The additional binding sites for podoplanin are Tyr153 and His154 and for sialylated O-glycan of podoplanin are Asn105, His119 and Tyr129 (Nagae et al., 2014).

2.5 | Human washed platelet preparation

Whole blood was collected from consenting, drug free donors using protocols approved by the University of Reading Ethics Committee. Healthy donors were aged between 20 and 50 years of age and both males and female. Washed platelets were prepared as previously described and resuspended in Tyrode's-HEPES buffer (134-mM NaCl, 2.9-mM KCl, 0.34-mM Na_2HPO_4 $12H_2O$, 12-mM $NaHCO_3$, 20-mM HEPES, 1-mM $MgCl_2$ and 5-mM glucose, pH 7.3) (Kempster et al., 2022).

2.6 | Light transmission aggregometry

Platelet aggregation was assessed using light transmission aggregation (AggRAM, Helena Biosciences). Washed platelets (2.5×10^8 cell per millilitre) were incubated with the inhibitor or vehicle control 5 min prior to the addition of agonist under stirring conditions (1200 rpm at 37°C). After agonist addition, platelet aggregation was monitored for 5 min.

2.7 | Platelet Signalling

Human washed platelets (8×10^8 cells per millilitre) were prepared under nonaggregating conditions (9-μM Integrilin) in the presence of secondary mediator inhibitors (10 μM indomethacin and 2 $U \cdot ml^{-1}$ apyrase) for CRP-XL stimulations or absence of secondary mediator inhibitors for rhodocytin stimulations. Stimulations were performed under stirring conditions (1200 rpm) for the indicated time point. Stimulations were stopped by the addition of one volume of ice-cold 2× lysis buffer (0.3-M sodium chloride; 20-mM Tris; 2-mM EGTA; 2-mM EDTA; 2% (v/v) NP-40; 10 $\mu g \cdot ml^{-1}$ aprotinin; 1 $\mu g \cdot ml^{-1}$ pepstatin; 10 $\mu g \cdot ml^{-1}$ leupeptin; 400 $\mu g \cdot ml^{-1}$ AEBFS; 5-mM sodium orthovanadate; pH 7.5). Samples were separated using SDS-PAGE and analysed by western blotting for total tyrosine phosphorylation and Syk tyrosine phosphorylation (525/526). Total Syk and GAPDH were used as loading controls. Primary antibodies were used at 1:1000 in 5% (w/v) BSA in TBS-T and reused up to five times. HRP-conjugated goat anti-rabbit and goat anti-mouse were used as secondary antibodies (1:5000 in TBS-T). A clear inhibition in CLEC-2 signalling in the presence of MAS9 was hypothesised. Given the predicted low variability, n = 3 was planned as part of the experimental design and provides qualitative insight to the action of MAS9.

2.8 | Flow cytometry

In a V-bottom 96-well platelet, 5 μl of washed platelets (4×10^8 cells per millilitre) were incubated with increasing concentrations of MAS9 (10, 20 and 30 μM) or DMSO vehicle control (0.3% [v/v]) for 5 min in the presence of Alexa Fluor 488-conjugated fibrinogen (100 $\mu g \cdot ml^{-1}$ final) and PE/Cy5 anti-human P-selectin (1:100) in a final volume of 50 μl. Platelets were then stimulated with 100-nM rhodocytin or 3 $\mu g \cdot ml^{-1}$ CRP-XL for 20 min in the dark. EDTA (10-μM final) and isotype control antibody (1:100) were used as a negative control for fibrinogen binding and P-selectin exposed, respectively. Samples were then fixed with 0.2% formyl saline and samples analysed using a BD Accuri C6 plus flow cytometer. A gate was applied around the platelets and 10,000 events collected.

2.9 | Platelet spreading and staining

Washed platelets (2×10^7 cell per millilitre) were spread on 300-nM rhodocytin, 10 $\mu g \cdot ml^{-1}$ recombinant podoplanin, 3 $\mu g \cdot ml^{-1}$ CRP-XL or 100 $\mu g \cdot ml^{-1}$ fibrinogen coated on to ø 13 mm glass coverslips. Coverslips were prepared by coating the coverslips overnight at 4°C. Following three washes with PBS (10-mM Na_2HPO_4, 1.8-mM KH_2PO_4, 2.7-mM KCl and 137-mM NaCl, pH 7.4) coverslips were blocked with 5 $mg \cdot ml^{-1}$ heat denatured BSA/PBS for 1 h at room temperature. Platelets were then fixed using formalin solution, 10% neutral buffered, for 10 min at room temperature, washed three times using PBS and permeabilised using 0.1% Triton X-100/PBS for 5 min at room temperature prior to labelling with Alexa Fluor 647 conjugated phalloidin (1:100 dilution in 5 $mg \cdot ml^{-1}$ heat denatured BSA/PBS) at room temperature for 1 h before mounting onto glass slides using Hydromount and imaged using a Nikon Eclipse Ti2 inverted microscope with HP Plan Apo VC 100× objective and Nikon DS-Qi2 camera. A clear inhibition in adhesion of platelets to podoplanin in the presence of MAS9 was hypothesised. Given the predicted low variability, n = 4 was planned as part of the experimental design and provides qualitative insight to the action of MAS9.

2.10 | Cell culture

Human dermal lymphatic endothelial cells (PromoCell RRID:SCR_023579, Cat# C-12216) were cultured in complete Endothelial cell growth medium MV2 (PromoCell) and used within five passages.

2.11 | Platelet spreading assay on HDLECs

Glass coverslips (ø 13 mm) were sterilised with 70% (v/v) ethanol and placed in each well of a 24-well plate; 1×10^5 of HDLECs were harvested in each well and cultured until 90%–100% confluency. On the day of the experiment, cell medium was removed and the cells were washed three times with PBS, before adding 300 μl of washed platelets at $2 \times 10^7 \cdot ml^{-1}$, pretreated with an inhibitor or 0.3% (v/v) DMSO final for 5 min. Cells with platelets were incubated for 45 min at 37°C. Non adherent platelets were removed by washing three times with DPBS and coverslips were fixed with 300 ml of Formalin Solution, 10% neutral buffered for 10 min, washed three times with 1× PBS and permeabilised with 300 μl of 0.1% (v/v) Triton-X100 for another 10 min. The coverslips were washed three times with PBS, stained with anti-podoplanin (NZ-1, 1:200) and APC conjugated anti-human CD42b antibodies (1:400) diluted in 5 $mg \cdot ml^{-1}$ heat denatured BSA/PBS. The excess of the antibodies was removed by washing three times with PBS. Afterwards, coverslips were incubated with Alexa Fluor 488 conjugated anti-rat antibody (1:1000 in PBS), as a secondary antibody to stain anti-podoplanin (NZ-1). The coverslips were washed three times with PBS, then three times with distilled water and mounted on 75 mm × 25 mm microscope slides using Hydromount.

2.12 | Immunofluorescence

Microscope slides from platelet spreading assays on immobilised agonists were imaged using an Eclipse Ti2 Inverted Microscope with HP Plan Apo VC 100×H objective and Camera Nikon DS-Qi2. DIC and epifluorescence pictures were taken with a frame size of 2424 × 2424 pixels (0.07 μm/px). Platelet spreading analysis was performed manually by counting the number of platelets in the field of view or, to determine the platelet surface area, by drawing the platelets and measuring them using the measure function in ImageJ (Fiji, version 1.53c). Platelet adhesion on HDLECs was imaged using a Nikon A1R confocal microscope using a Plan Apo λ 100× oil objective. The immuno-related procedures used comply with the recommentations made by the British Journal of Pharmacology.

2.13 | Data and statistical analysis

The data and statistical analysis comply with the British Journal of Pharmacology recommendations on experimental design and analysis in pharmacology (Curtis et al., 2022). Randomisation was applied to all platelet assays, with conditions randomly applied. Blinding was either performed at the point of data collection or at the point of analysis.

All data are presented as the mean ± standard deviation. Where indicated, statistical analysis was performed using unpaired two tailed *t*-test or one-way ANOVA. One-way ANOVA was performed when three or more groups were compared for one variable (univariate comparisons), followed if significant by Dunnett's post hoc multiple comparisons. Statistical significance represented by $^*P \leq 0.05$. All statistical analyses were performed using GraphPad Prism 7. Single values (n) represent independent biological replicates.

2.14 | Nomenclature of targets and ligands

Key protein targets and ligands in this article are hyperlinked to corresponding entries in https://www.guidetopharmacology.org and are permanently archived in the Concise Guide to PHARMACOLOGY 23/24 (Alexander et al., 2021).

3 | RESULTS

3.1 | Primary high-throughput screen (HTS) and inhibitor identification

An AlphaScreen assay was developed and optimised for a HTS to identify inhibitors of the CLEC-2–podoplanin interaction. We employed donor beads, which contain a photosensitiser phthalocyanine that converts oxygen into a singlet form after illumination at 680 nm. These donor beads were coated with monobiotinylated recombinant podoplanin. When in close proximity (<200 nm) to HIS-tagged recombinant CLEC-2-coated acceptor beads, the energy of the singlet oxygen is transferred to thioxene, generating a fluorescent signal between 520 and 620 nm. If the proximity of the donor and acceptor beads is disrupted, the singlet oxygen returns to its ground state and no signal is generated (Peppard et al., 2003). The overall principle of the AlphaScreen assay is summarised in Figure 1a.

Using a 1536-well format, 18,476 small molecules were tested. All plates were validated with a signal-to-background (S/B) ratio greater than 8.49 and *Z′* values above 0.58; 14 compounds presented with a greater than 50% inhibition at a concentration of 5 μM. These compounds were taken forward for secondary screening (Figure 2, Table S1). Based on their structures, five compounds from the

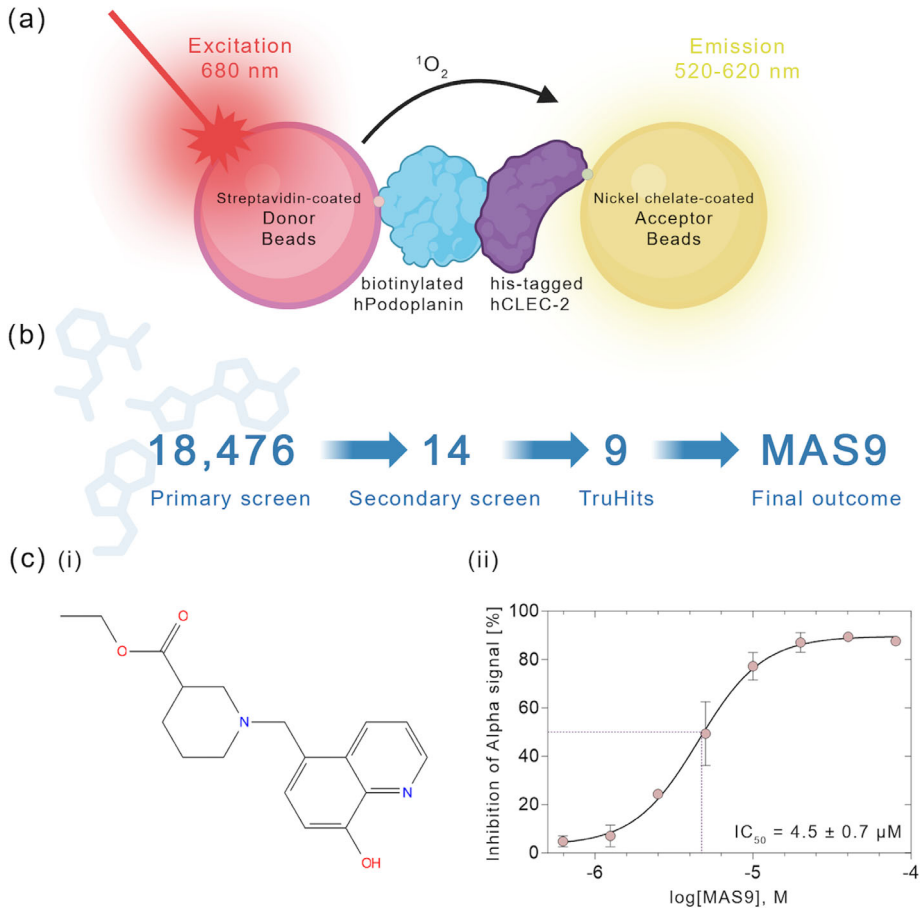

FIGURE 1 AlphaScreen identifies MAS9 as an inhibitor of the CLEC-2–Podoplanin interaction. (a) Schematic diagram of the AlphaScreen assay. Excitation at a wavelength of 680-nm results in the conversion of oxygen to an excited singlet oxygen by the donor bead (coated with streptavidin/biotinylated human Podoplanin). If the donor bead is in close proximity (∼200 nm) to the acceptor bead (nickel chelate beads coated with HIS-tagged hCLEC-2), the singlet oxygen excites the acceptor bead resulting in light emission at 520–620 nm. Inhibiting the interaction between the donor and acceptor beads results in lower or no emission. (b) Summary of the identification process. A total of 18,476 molecules were screened using a high-throughput AlphaScreen. A secondary screen and cytotoxicity assays resulted in the identification of one small molecule, MAS9. (c) (i) Structure of MAS9. (ii) dose–response curve for MAS9 (concentration range 160–0.3125 μM) to determine its IC_{50} value. Data are shown as mean ± standard deviation.

	(a)	(b)	(c)	(d)	(e)
Compound name	Primary screening inhibition [%]	Secondary screening inhibition [%]	Singlet oxygen quenchers, colour quenchers, or light-scattering agents	Biotin mimetics	Soluble in non-organic solvents
Clofazimine	84	-	-	-	-
Mitoxantrone dihydrochloride	86	-	-	-	-
Biotin	104	-	-	-	-
Lorglumide sodium salt	78	-	-	-	-
Anthralin	105	-	-	-	-
MAS1	89	5.8	No	-	-
MAS2	74	0	No	-	-
MAS3	91	0	No	-	-
MAS4	80	83	No	No	No
MAS5	75	0	Yes	-	-
MAS6	64	28	Yes	-	-
MAS7	105	0	No	-	-
MAS8	57	33.9	Yes	-	-
MAS9	92	80.9	No	No	Yes

FIGURE 2 Legend on next page.

Prestwick library were excluded due to likely false positive inhibition. Of the remaining nine novel small molecules, seven were excluded as singlet oxygen quenchers, colour quenchers, light scattering agents or biotin mimetics when using an AlphaScreen TruHits assay, or did not present with reproducible inhibition (Table S2). One further compound was excluded due to poor solubility in a range of buffers. The hit compound identification workflow is summarised in Figure 1b and an overview of all hit compounds, including justifications for the exclusion of individual compounds for further testing, is summarised in Figure 2. The remaining novel small molecule compound, ethyl 1-[(8-hydroxy-5-quinolinyl)methyl]-3-piperidinecarboxylate, here termed MAS9, was taken forward for further characterisation (Figure 1c(i)).

A dose–response study determined the IC_{50} value of MAS9 as 4.5 ± 0.7 μM and guided the range of concentrations used during further characterisation of the compound (Figure 1c(ii)). Using a calcein retention assay, MAS9 demonstrated no platelet toxicity up to the tested concentration of 30 μM (Figure S2).

3.2 | In silico modelling of the MAS9–CLEC-2 interaction

Directed molecular docking was used to predict the preferential binding mode of MAS9 to the extracellular domain of CLEC-2. The crystal structure of CLEC-2 was first refined by optimising hydrogen bonding, adding in missing hydrogens, removal of water molecules beyond 5 Å from nonstandard residues and generating the ionisation states at pH 7.0 ± 2.0. The MAS9 ligand was prepared by generating possible tautomers and different protonation states, and minimised in the CLEC-2 field using a standard molecular mechanics energy function in conjunction with a distance dependent dielectric model. Docking analysis predicts that the S configuration of MAS9 ((S)-ethyl 1-[(8-hydroxy-5-quinolinyl)methyl]-3-piperidinecarboxylate) binds to Arg107, Arg 152, Thr153 and Arg157 by hydrogen bonding and creates a noncovalent interaction, using π-π stacking, between the aromatics ring of MAS9 and His154 of CLEC-2 (Figure 3). The predicted glide score for this docking pose was -3.576 kcal·mol^{-1}. Docking analysis of the R configuration of MAS9 ((R)-ethyl 1-[(8-hydroxy-5-quinolinyl)methyl]-3-piperidinecarboxylate) binds to Arg107 and Arg152 by hydrogen bonds (Figure S3). The predicted glide score was lower than for the (S)- enantiomer at -3.27 kcal·mol^{-1}.

3.3 | MAS9 inhibits CLEC-2-mediated platelet aggregation

To investigate the effect of MAS9 on CLEC-2-mediated platelet aggregation, washed platelets were preincubated either with increasing concentrations of MAS9 or vehicle control prior to the addition of 30-nM rhodocytin or 5 μg·ml^{-1} hemin; 20- and 30-μM MAS9 significantly inhibited platelet aggregation to both CLEC-2 agonists (Figure 4a,b). The inhibitory effect of MAS9 could be overcome by higher concentrations of rhodocytin (100 nM) but was maintained for a higher concentration of hemin (10 μg·ml^{-1}) (Figure S4). MAS9 had no inhibitory effect either on 0.3 μg·ml^{-1} CRP-XL or 0.1 U·ml^{-1} thrombin-mediated platelet aggregation (Figure 4c). MAS9 also had no inhibitory effect on lower concentrations of thrombin or U46619-mediated aggregation (Figure S5).

3.4 | MAS9 inhibits CLEC-2-mediated signalling

To investigate the effect of MAS9 on CLEC-2-mediated signalling, washed platelets, under nonaggregating conditions, were incubated either with increasing concentrations of MAS9 or vehicle control prior the addition of 100-nM rhodocytin. Apyrase and indomethacin were omitted from rhodocytin stimulated samples because CLEC-2-mediated signalling requires secondary mediators to reinforce its signalling (Pollitt et al., 2010). Exploratory data suggests that 20- and 30-μM MAS9 inhibited total cell tyrosine phosphorylation (Figure 5a), CLEC-2 tyrosine phosphorylation (Figure S6) and Syk tyrosine phosphorylation at positions Y525/Y526 following rhodocytin stimulation (Figure 5b). MAS9 had no inhibitory effect on CRP-XL-mediated total tyrosine phosphorylation or Syk tyrosine phosphorylation at positions Y525/Y526 (Figure 5a,c).

3.5 | MAS9 inhibits CLEC-2-mediated fibrinogen binding and P-selectin exposure

To investigate the effect of MAS9 on integrin $\alpha_{IIb}\beta_3$ activation and granule release downstream of CLEC-2-mediated platelet activation, washed platelets were stimulated with 100-nM rhodocytin in the presence and absence of MAS9. Fibrinogen binding and P-selectin exposure were assessed using flow cytometry to measure integrin activation and granule release respectively. Of note, unlike 100 nM of rhodocytin, 30 nM

FIGURE 2 Selection of MAS9 as a lead compound to study its inhibitory effect of the CLEC-2–Podoplanin interaction. (a) Inhibitory effect of the compounds at a concentration of 5 μM in the primary high-throughput screening [%]. (b) Inhibitory effect of the compounds at a concentration of 20 μM in the secondary screening [%]. Five compounds (1–5) have been excluded from secondary screening based on their chemical structure. (c) Determination using AlphaScreen™ TruHits™ assay for MAS1–9 which of the compounds interfere with AlphaScreen assay (singlet oxygen quenchers, colour quenchers or light-scattering agents). (d) Determination using AlphaScreen™ TruHits™ assay for MAS4 and MAS9 if the compound is the biotin mimetic. (e) Visual inspection of MAS4 and MAS9 if the compound is soluble in nonorganic solvents by diluting DMSO stock in PBS, HEPES buffer (range of pH) or water. (a–e) The colours in the figure indicate if the compound passed the test or not. The green colour indicates that the compound passed the test; the red colour indicates that the compound did not pass the test.

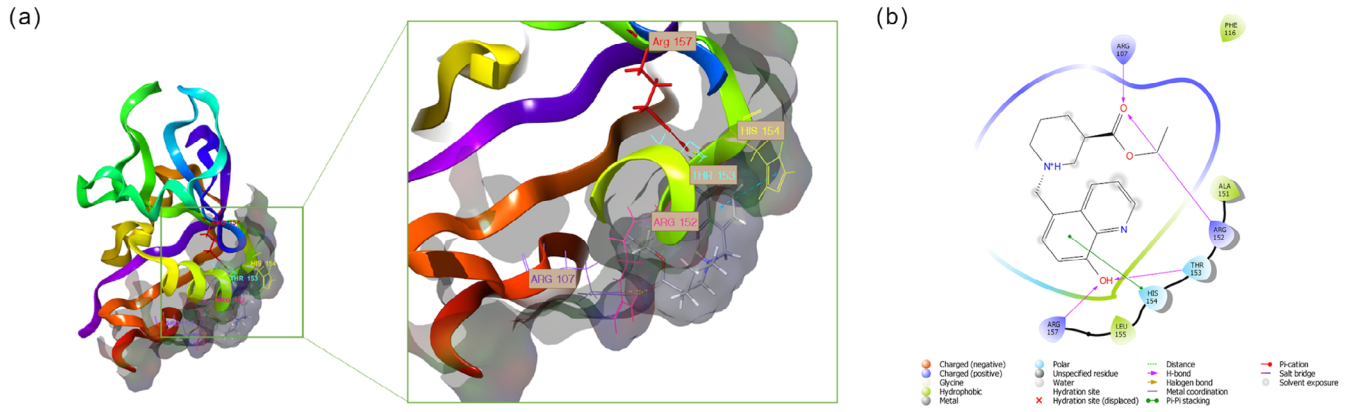

FIGURE 3 Modelling the interaction of MAS9 with human CLEC-2. (a) Three-dimensional visualisation of the binding of MAS9 docked to the structure of human CLEC-2. (b) Two-dimensional diagram of MAS9 binding to CLEC-2. MAS9 is shown as a stick diagram. H-bonds between the MAS9 and CLEC-2 are shown as purple lines. π-π stacking interaction is shown in green.

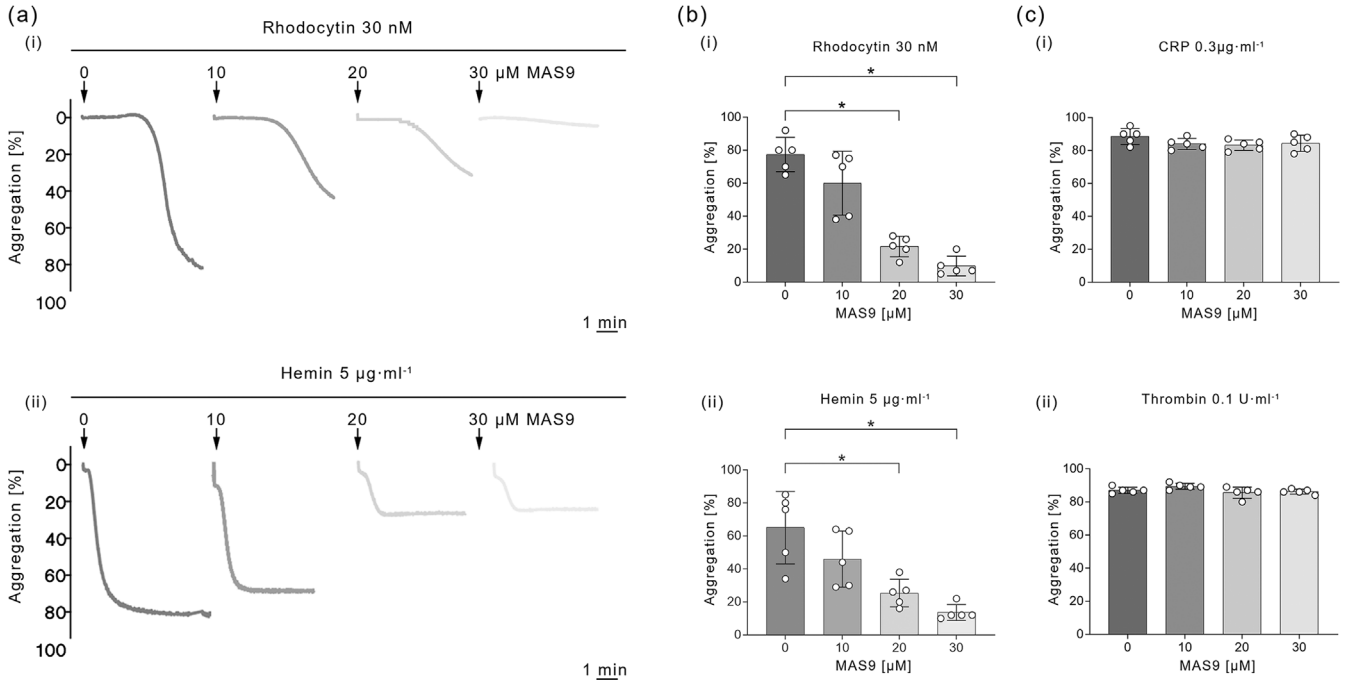

FIGURE 4 MAS9 inhibits CLEC-2-mediated aggregation. (a) Representative aggregation traces induced by (i) 30-nM rhodocytin (ii) 5 μg·ml^{-1} hemin in the presence of increasing concentration of MAS9. (b) Quantification of the percentage aggregation induced by (i) 30-nM rhodocytin (ii) 5 μg·ml^{-1} hemin in the presence of increasing concentration of MAS9 compared with the vehicle control (0.3% [v/v] DMSO). (c) Quantification of the percentage aggregation induced by (i) 0.3 μg·ml^{-1} CRP-XL (ii) 0.1 U·ml^{-1} thrombin in the presence of increasing concentration of MAS9 compared with the vehicle control (0.3% [v/v] DMSO). Statistical significance was calculated using one-way ANOVA with Dunnett's post-test. Data shown as the mean ± standard deviation (n = 5) $^*P \leq 0.05$.

of rhodocytin did not result either in integrin activation or P-selectin exposure. 30 μM of MAS9 significantly inhibited fibrinogen binding (Figure 6a(i)) and P-selectin exposure (Figure 6b(i)) downstream of 100 nM rhodocytin stimulation. Lower concentrations of MAS9 (10 and 20 μM) had no effect on fibrinogen binding and P-selectin exposure downstream of rhodocytin stimulation (Figure 6a(i),b(i)). MAS9 also had no effects on rhodocytin-induced fibrinogen and P-selectin exposure in platelet-rich plasma (Figure S7). This outcome suggests that MAS9 is not bioavailable in plasma. Unexpectedly, MAS9 inhibited CRP-XL-mediated fibrinogen binding in a concentration-dependent manner (Figure 6a(ii)). However, MAS9 had no effect on P-selectin exposure downstream of CRP-XL stimulation (Figure 6b(ii)).

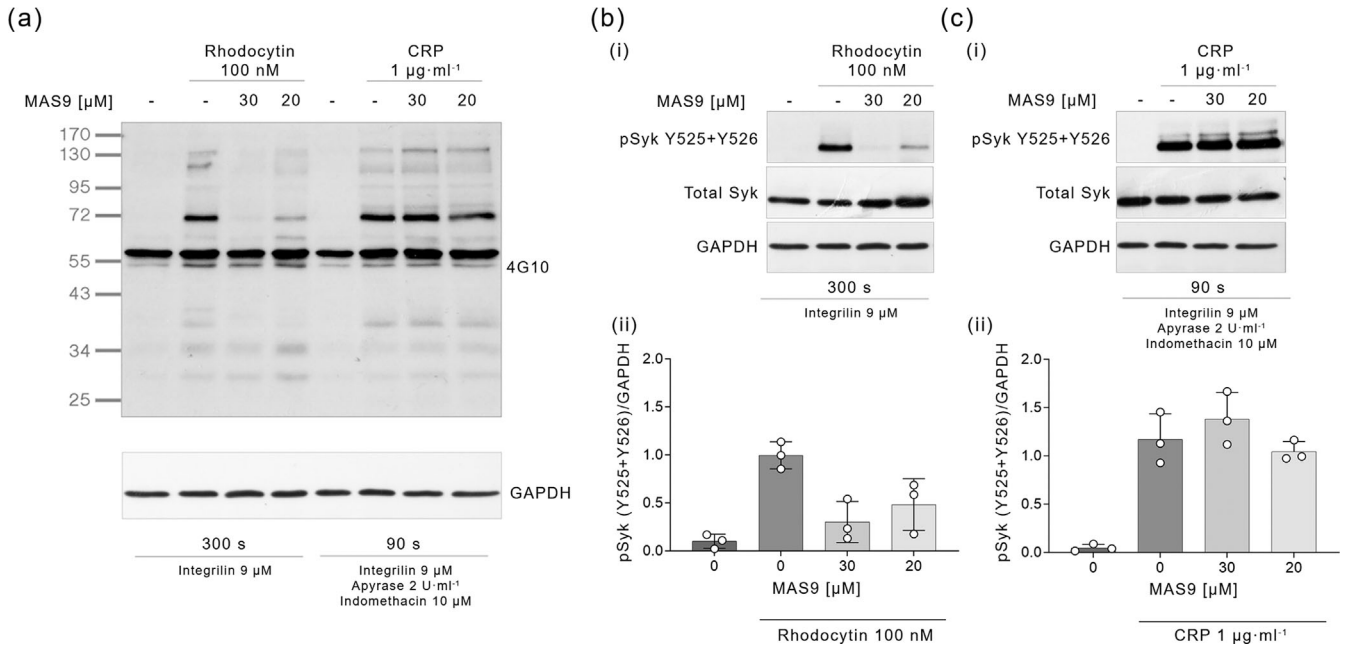

FIGURE 5 MAS9 inhibits CLEC-2-mediated signalling. Washed platelets (8×10^8·ml^{-1}) in the presence of 9-μM integrilin for the rhodocytin stimulations and 2 U·ml^{-1} apyrase, 10 μM indomethacin and 9-μM integrilin for the CRP-XL stimulations were pretreated with MAS9 (20 or 30 μM) or vehicle control (0.3% [v/v] DMSO) for 10 min before stimulation with 100-nM rhodocytin or 1 μg·ml^{-1} CRP-XL. Lysates were separated by SDS-PAGE and analysed by western blotting for (a) tyrosine-phosphorylated proteins (4G10), (b,c) phospho-Syk (Y525/526). GAPDH and total Syk were used as loading controls. Representative blots n = 3.

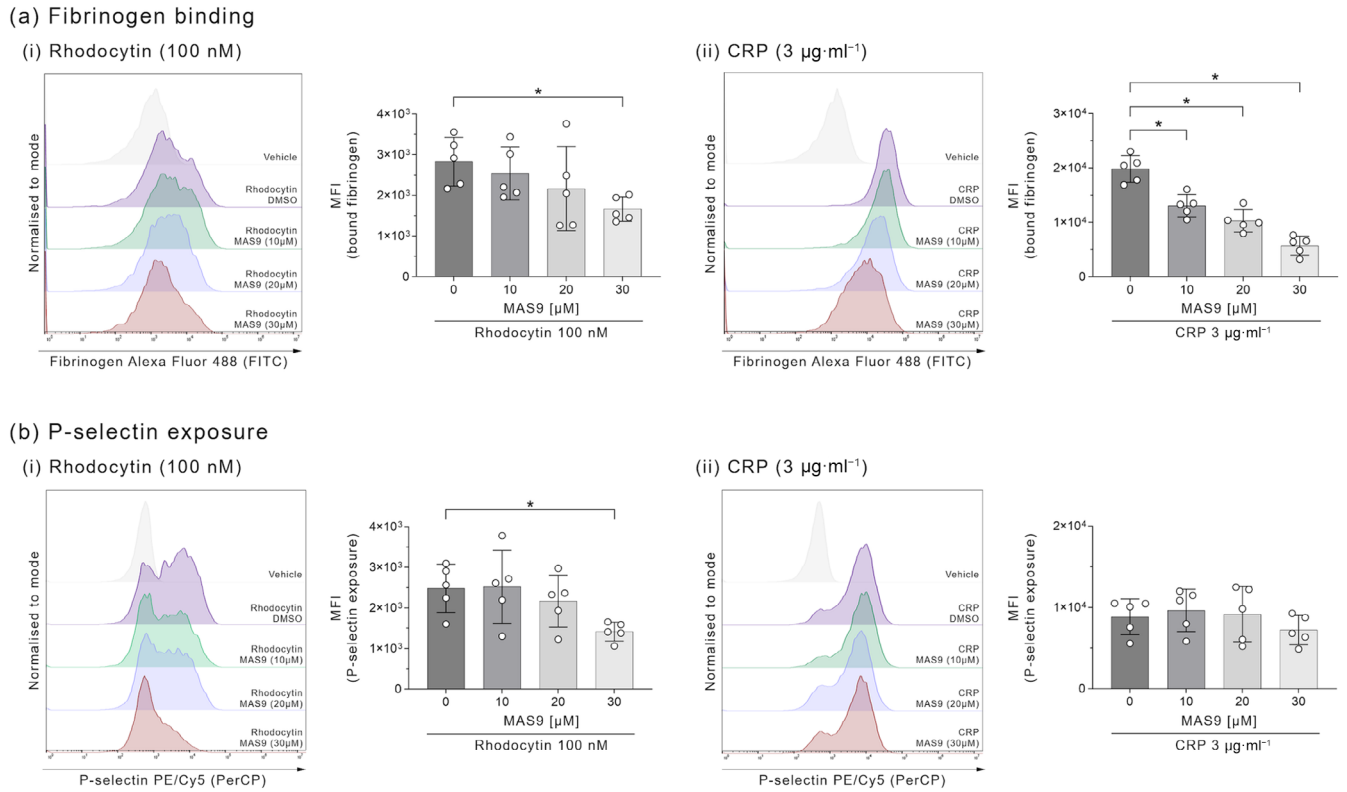

FIGURE 6 MAS9 inhibits P-selectin and fibrinogen binding. Washed platelets (4×10^8 cells per millilitre) were incubated with MAS9 (10, 20 or 30 μM) or vehicle control (0.3% [v/v] DMSO) for 5 min with the addition of Alexa Fluor 488-conjugated fibrinogen to measure (a) fibrinogen binding and PE/Cy5 anti-human CD62P antibody to measure (b) P-selectin exposure prior to stimulation with (i) 100-nM rhodocytin or (ii) 3 μg·ml^{-1} CRP-XL. Data presented as the median fluorescence intensity. Statistical significance was calculated using one-way ANOVA with Dunnett's post-test. Data shown as the mean ± standard deviation (n = 5) *$P \leq 0.05$.

3.6 | MAS9 inhibits CLEC-2-dependent platelet adhesion but inhibits platelet spreading to all substrates

The experiments described above were performed using soluble ligands; however, the endogenous ligand of CLEC-2, podoplanin, is found at the surface of cells rather than in a soluble form. To determine the impact of MAS9 on the interaction of platelets with immobilised ligands, platelets were allowed to adhere to ligands immobilised to glass coverslips. To determine whether MAS9 had an inhibitory effect on CLEC-2-mediated platelet spreading, platelets were allowed to adhere to immobilised 300-nM rhodocytin and 10 $\mu g \cdot ml^{-1}$ recombinant podoplanin in the presence and absence of MAS9. Exploratory data suggests that platelet incubation with MAS9 inhibited platelet adhesion and spreading to rhodocytin or podoplanin in a concentration-dependent manner (Figure 7a(i–iii),b(i–iii)).

To determine the selectivity of MAS9 for CLEC-2, platelets were allowed to interact with other agonists, including 3 $\mu g \cdot ml^{-1}$ CRP-XL and 100 $\mu g \cdot ml^{-1}$ fibrinogen; 10 and 20 μM of MAS9 did not inhibit platelet adhesion to CRP-XL; however, a decrease in the adhesion of platelets to CRP-XL was observed in the presence of 30-μM MAS9 (Figure 7c(ii)). MAS9 did not inhibit platelet adhesion to fibrinogen (Figure 7d(ii)). Nonetheless, a concentration-dependent inhibition of platelet spreading on CRP-XL and fibrinogen was observed (Figure 7c(iii),d(iii)).

3.7 | MAS9 inhibits platelet adhesion to podoplanin expressing lymphatic endothelial cells

To determine how MAS9 effects the interaction of platelets with a physiologically expressed ligand, platelets were incubated with a monolayer of human dermal lymphatic endothelial cells (HDLECs), which endogenously express podoplanin (Breiteneder-Geleff et al., 1999). Foci of podoplanin, which colocalised with platelets, were observed in the vehicle control. These foci were lost in the presence of increasing concentrations of MAS9 (Figure 8a). Platelet adhesion to HDLECs was inhibited in a concentration-dependent manner in the presence of MAS9 (Figure 8b). To investigate the accumulation of membrane-associated podoplanin as foci at the interface between the platelets and lymphatic endothelial cells, Z-stack images were taken. The Z projection shows the accumulation of podoplanin at the interface between the platelets and the lymphatic endothelial cells. This accumulation is lost in the presence of MAS9 (Figure 8c).

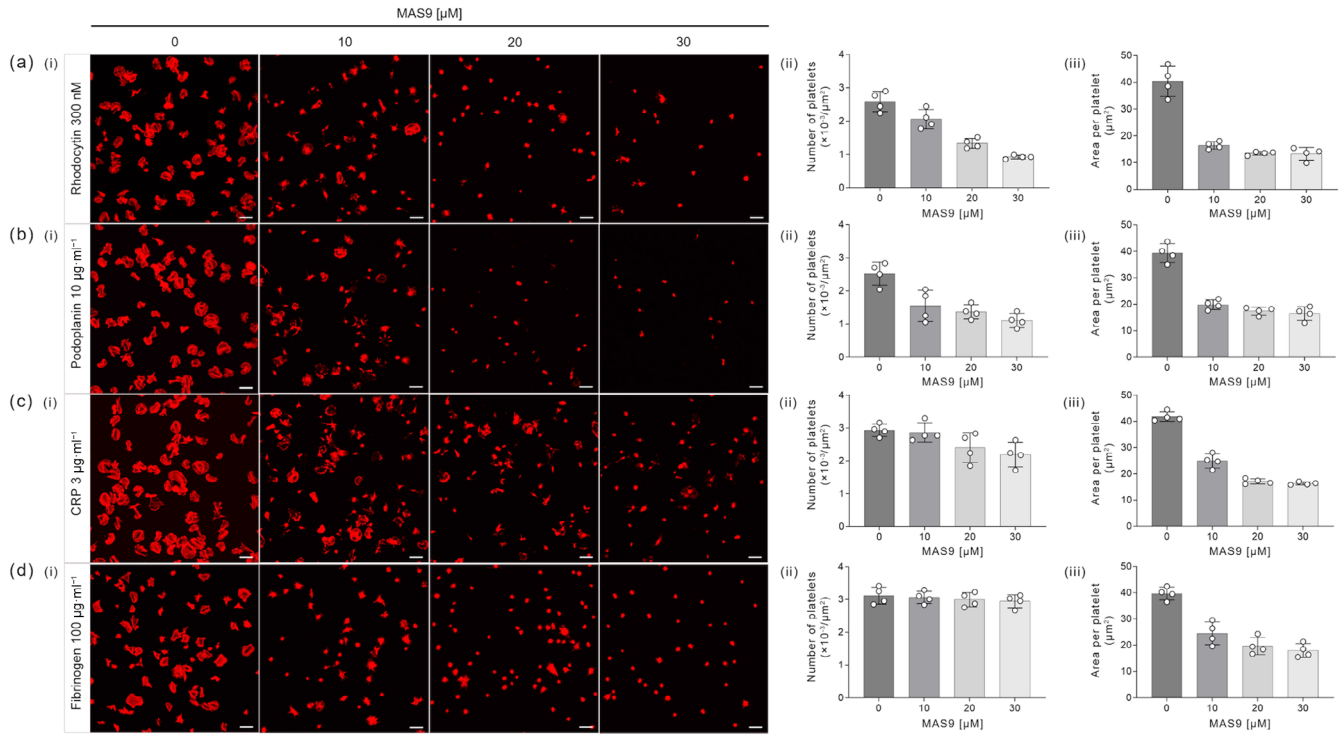

FIGURE 7 MAS9 inhibits adhesion and spreading of platelets to CLEC-2 ligands but inhibits platelet spreading on all substrates. Washed platelets (2×10^7 cells per millilitre) were incubated with MAS9 (10, 20 or 30 μM) or vehicle control (0.3% v/v DMSO) for 5 min before being spread over (a) rhodocytin (300 nM), (b) recombinant podoplanin (10 $\mu g \cdot ml^{-1}$), (c) CRP-XL (3 $\mu g \cdot ml^{-1}$) and (d) fibrinogen (100 $\mu g \cdot ml^{-1}$) for 45 min at 37°C. (i) Representative images of platelets spread on the indicated substrate in the presence of MAS9 or vehicle control (0.3% [v/v] DMSO). Scale bar 10 μm. (ii) quantification of platelet adhesion. (iii) Quantification of platelet spread area. Data shown as the mean ± standard deviation ($n = 4$).

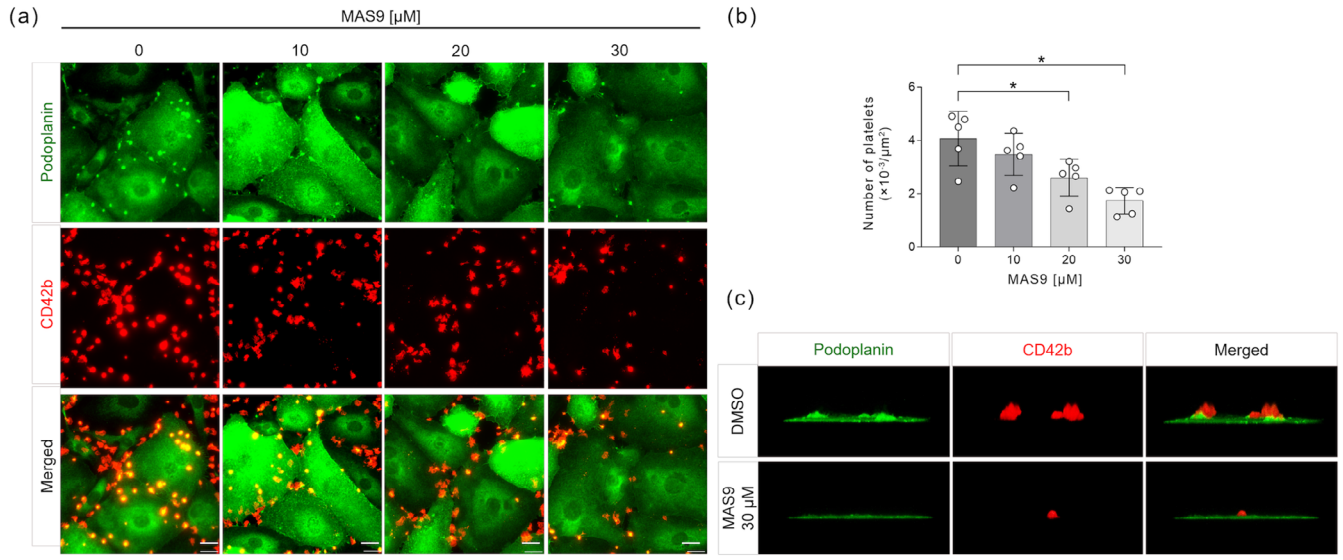

FIGURE 8 MAS9 inhibits platelet adhesion to human dermal lymphatic endothelial cells. Washed platelets (2×10^7 cells per millilitre) were incubated in the presence of MAS9 (10, 20 or 30 μM) or vehicle control (0.3% [v/v] DMSO) for 5 min before incubation with human dermal lymphatic endothelial cells (HDLECs) for 45 min at 37°C. Cells were then fixed, permeabilised and stained with anti-podoplanin and anti-CD42b antibodies. (a) Representative images of platelets adhered to HDLECs. HDLECs stained for podoplanin and platelets stained with CD42b (platelet glycoprotein Ib). Accumulation of podoplanin at the interface between the platelets and HDLECs is indicated by white arrows. Scale bar 10 μm. (b) Z projection of platelets interacting with HDLECs. (c) Quantification of the number of platelets adhered per HDLEC area in the presence or absence of MAS9. Statistical significance was calculated using one-way ANOVA with Dunnett's post-test. Data shown as the mean ± standard deviation. *$P \leq 0.05$ ($n = 5$).

4 | DISCUSSION

We identified MAS9 as a candidate novel small molecule inhibitor of the CLEC-2–podoplanin interaction using an AlphaScreen high-throughput assay. From 18,476 compounds, 14 presented with greater than 50% inhibition. This represents a hit rate of 0.075%. This is a rate typically achieved by HTS, with rates reported in the range of 0.01%–0.14% (Zhu et al., 2013). Following secondary screening, MAS9 was identified as an inhibitor of the CLEC-2–podoplanin interaction, but did not have cytotoxic effects on platelets, and was taken forward for further characterisation. MAS9 fulfils the criteria of a drug-like compound as described by Lipinski's rule of 5 (Lipinski et al., 2001). It has a molecular weight of 314.38 Da, an octanol–water partition coefficient (log P) of 2.73, has a single H-bond donor and four H-bond acceptors. MAS9 has several functional groups, including an ester and a phenolic hydroxy group. These functional groups have the potential to affect the absorption, distribution, metabolism and excretion (ADME) profile of MAS9. In addition to influencing the pharmacokinetics of MAS9, these functional groups may impact the pharmacodynamics of MAS9.

While we did not identify MAS9 as a false positive compound in an AlphaScreen TruHits assay, it has been identified as a potential compound that can optically interfere with the AlphaScreen assay in another study (NCBI, 2024a). However, it was identified as inactive in another AlphaScreen by the same institute (NCBI, 2024b). It is unclear why there are these discrepancies in assay outcomes but it may be a result of different reaction buffers, experimental design and conditions used in each screen. A significant difference between these studies, and the one presented here is that a counter screen was used in the former studies rather than a TruHits assay presented here. The TruHits assay specifically identifies compounds that interfere with the AlphaScreen technology. In silico modelling suggests that MAS9 interacts with three of the four arginine residues in the overlapping CLEC-2 binding site of podoplanin and rhodocytin (Arg107, Arg152 and Arg157) (Nagae et al., 2014). The additional site of the MAS9 interaction with CLEC-2 is via π-π stacking to His154, which is important for the interaction of podoplanin with CLEC-2 (Nagae et al., 2014). The binding sites of MAS9 to CLEC-2 share similarities to another known CLEC-2 inhibitor, 2CP (Chang et al., 2015). Molecular docking of 2CP to CLEC-2 identified interactions with Asn105, Arg107, Phe116, Arg188 and Arg157 of CLEC-2. Many of these sites correspond to binding sites for podoplanin and rhodocytin. The other small molecule CLEC-2 inhibitor, cobalt hematoporphyrin, interacts with residues not common to the CLEC-2 binding site of podoplanin and rhodocytin (Tsukiji et al., 2018). This last finding suggests that the inhibitory effect of cobalt hematoporphyrin may be by an allosteric mechanism. A CLEC-2 mutagenesis study may support the identification of the MAS9 binding site.

In this study, MAS9 was shown to inhibit hemin-induced platelet aggregation. The binding site of hemin is not yet known. Interestingly, hemin-induced platelet aggregation cannot be blocked by the CLEC-2 blocking antibody AYP1 (Bourne et al., 2021). This observation provides indirect evidence that hemin binds to a distinct site on CLEC-2 than podoplanin.

The IC_{50} value determined using the AlphaScreen was 4.5 ± 0.7 μM; however, higher concentrations were needed to inhibit CLEC-2-mediated functions. This difference in potency likely reflects the differences between cell-free and cell-based assays. In cell-based assays, MAS9 may be sequestered by cellular proteins, reducing the concentration of active compound. This conclusion is supported by the lack of activity of MAS9 in platelet-rich plasma. MAS9 displayed inhibition for CLEC-2-mediated aggregation over other platelet receptors, GPVI, **thromboxane prostanoid (TP) receptor**, and **proteinase activated receptors** (PAR1 and PAR4). MAS9 also displayed selective inhibition of CLEC-2-mediated tyrosine kinase signalling. CLEC-2 and GPVI share similar proximal signalling events, including the phosphorylation and activation of the kinase Syk (Severin et al., 2011). MAS9 did not have any effect on Syk phosphorylation downstream of GPVI but resulted in reduced Syk phosphorylation downstream of CLEC-2. MAS9 also inhibited tyrosine phosphorylation of CLEC-2. Secondary mediators play a critical positive feedback role in mediating human CLEC-2 phosphorylation. When secondary mediators are inhibited, CLEC-2 phosphorylation is lost (Pollitt et al., 2010). The inhibition of downstream signalling events in the presence of MAS9 may contribute to reduced levels of CLEC-2 phosphorylation.

Interestingly, MAS9 inhibited fibrinogen binding downstream of GPVI stimulation when assessed by flow cytometry. MAS9 also inhibited the spreading of platelets to fibrinogen, but not adhesion. This raises the possibility of integrin–hemITAM interactions and/or receptor crosstalk. There is a precedent for this concept, with evidence supporting crosstalk between integrins and ITAM-bearing receptors. A functional relationship between the integrin $\alpha_{IIb}\beta_3$ and the ITAM-bearing receptor **FcγRIIA** has been observed. Blocking FcγRIIA, to prevent ligand binding, has been shown to inhibit spreading of platelets, but not adhesion to immobilised fibrinogen, suggesting a link between outside-in integrin signalling and ITAM-mediated signalling (Boylan et al., 2008). However, it is possible that these outcomes are caused by nonspecific actions of MAS9.

MAS9 also inhibited platelet spreading on CRP-XL. Platelets secrete fibrinogen following activation. Platelets may go on to bind the fibrinogen released from platelet granules during the activation and spreading process. Therefore, any potential inhibitory role of MAS9 on integrin–hemITAM interactions may lead to impaired platelet spreading. The impact of other CLEC-2 inhibitors, such as 2CP and cobalt hematoporphyrin, on fibrinogen binding has not been investigated in the literature. Therefore, it is unknown if this is a common finding amongst CLEC-2 inhibitors. Equally, CLEC-2 independent mechanisms of MAS9 on platelet function cannot be ruled out.

The CLEC-2–podoplanin interaction is important for cell–cell communication. MAS9 was demonstrated to inhibit the interaction of platelets with human dermal lymphatic endothelial cells (HDLECs), which endogenously express the CLEC-2 ligand podoplanin. In addition to inhibiting platelet adhesion to the lymphatic endothelial cells, MAS9 inhibited the formation of podoplanin foci at the interface between the platelets and the cell. Similar accumulation of podoplanin has been seen by mouse platelets interacting with mobile mouse podoplanin, with the formation of podoplanin clusters dependent on CLEC-2 (Pollitt et al., 2014). This suggests that the CLEC-2–podoplanin interaction drives the formation of podoplanin clustering and suggests a common mechanism between human and mouse. The regulation of podoplanin clusters may be regulated by protein partners. For example, the regulation and stability of podoplanin clustering by CLEC-2 has been proposed to be mediated by CD44 in fibroblastic reticular cells (Lim et al., 2023). However, lymphatic endothelial cells do not express CD44 and podoplanin may interact with other protein partners in different cell types to regulate clustering and downstream signalling.

In this study, MAS9 was characterised using human platelets. However, other cells such as megakaryocytes, dendritic and liver sinusoidal endothelial cells also express CLEC-2 (Nakamura-Ishizu et al., 2015; Suzuki-Inoue et al., 2011). The impact of MAS9 on other cellular processes would need to be assessed because future bioavailable derivatives of MAS9 may have the potential to impact physiological processes such as thrombocytopoiesis, haematopoiesis and lymphatic development (Nakamura-Ishizu et al., 2015; Tsukiji & Suzuki-Inoue, 2023). Although there was no cytotoxicity of MAS9 observed in platelets, the impact of MAS9 will need to be explored in other cell types. Since CLEC-2 is a C-type lectin, the impact of MAS9 on other lectins also needs to be investigated.

In summary, MAS9 has been identified as a candidate small molecule inhibitor for CLEC-2. This opens the door for future preclinical and clinical assays to explore the potential of MAS9 as a therapeutic compound for a variety of pathophysiological processes, including tumour metastasis, lymphatic vessel formation and thrombo-inflammation.

AUTHOR CONTRIBUTIONS

Marcin A. Sowa performed experimental work, and contributed to the design, analysis, curation and interpretation of the data. Marcin A. Sowa prepared the figures and tables and, along with Alice Y. Pollitt, wrote the initial draft. Yan Wu contributed to the experimental work. Jan van Groningen supported the development of the HTS. Ying Di and Johannes A. Eble provided reagents. Jan van Groningen, Helma van den Hurk, Jonathan M. Gibbins, Ángel García and Alice Y. Pollitt provided supervision support for the research. Helma van den Hurk, Jonathan M. Gibbins, Ángel García and Alice Y. Pollitt contributed to the acquisition of funding for the project leading to its publication. Marcin A. Sowa, Ángel García and Alice Y. Pollitt contributed to the conceptualisation of the study. All authors contributed to critical revision and final approval of the manuscript.

ACKNOWLEDGEMENTS

MAS was supported by the European Union's Horizon 2020 research and innovation program (Marie Sklodowska-Curie grant agreement No. 766118) to AG, AYP and JMG. YW was supported by the NC3Rs (NC/Y000870/1) to AYP. AYP acknowledges support by the Academy of Medical Science springboard award (SBF002\1099). AG acknowledges support by the Spanish Ministry of Science, Innovation and Universities (Grant No. PID2019-108727RB-I00 and PDC2022-133743-I00), co-funded by the European Regional

Development Fund (ERDF), and Next Generation EU funds. JAE is financially supported by the Deutsche Forschungsgemeinschaft (DFG) with grant Eb177/19-1 (project number: 414847370).

CONFLICT OF INTEREST STATEMENT

The authors have no conflict of interest to declare.

DATA AVAILABILITY STATEMENT

Data are available on request from the authors.

DECLARATION OF TRANSPARENCY AND SCIENTIFIC RIGOUR

This Declaration acknowledges that this paper adheres to the principles for transparent reporting and scientific rigour of preclinical research as stated in the *BJP* guidelines for Design and Analysis and Immunoblotting and Immunochemistry and as recommended by funding agencies, publishers and other organisations engaged with supporting research.

ORCID

Marcin A. Sowa https://orcid.org/0000-0003-0038-0122
Yan Wu https://orcid.org/0000-0002-0470-4908
Johannes A. Eble https://orcid.org/0000-0001-9156-2137
Jonathan M. Gibbins https://orcid.org/0000-0002-0372-5352
Ángel García https://orcid.org/0000-0003-1176-5917
Alice Y. Pollitt https://orcid.org/0000-0001-8706-5154

REFERENCES

Alexander, S. P., Kelly, E., Mathie, A., Peters, J. A., Veale, E. L., Armstrong, J. F., Faccenda, E., Harding, S. D., Pawson, A. J., Southan, C., Buneman, O. P., & Zolghadri, Y. (2021). The Concise Guide to PHARMACOLOGY 2021/22: Introduction and other protein targets. *British Journal of Pharmacology*, *178*(Suppl 1), S1–S26. https://doi.org/10.1111/bph.15537

Berridge, M. J., Bootman, M. D., & Roderick, H. L. (2003). Calcium signalling: Dynamics, homeostasis and remodelling. *Nature Reviews. Molecular Cell Biology*, *4*(7), 517–529. https://doi.org/10.1038/nrm1155

Bourne, J. H., Colicchia, M., Di, Y., Martin, E., Slater, A., Roumenina, L. T., Dimitrov, J. D., Watson, S. P., & Rayes, J. (2021). Heme induces human and mouse platelet activation through C-type-lectin-like receptor-2. *Haematologica*, *106*(2), 626–629. https://doi.org/10.3324/haematol.2020.246488

Boylan, B., Gao, C., Rathore, V., Gill, J. C., Newman, D. K., & Newman, P. J. (2008). Identification of FcgammaRIIa as the ITAM-bearing receptor mediating alphaIIbbeta3 outside-in integrin signaling in human platelets. *Blood*, *112*(7), 2780–2786. https://doi.org/10.1182/blood-2008-02-142125

Breiteneder-Geleff, S., Soleiman, A., Kowalski, H., Horvat, R., Amann, G., Kriehuber, E., Diem, K., Weninger, W., Tschachler, E., Alitalo, K., & Kerjaschki, D. (1999). Angiosarcomas express mixed endothelial phenotypes of blood and lymphatic capillaries: Podoplanin as a specific marker for lymphatic endothelium. *The American Journal of Pathology*, *154*(2), 385–394. https://doi.org/10.1016/S0002-9440(10)65285-6

Chang, Y. W., Hsieh, P. W., Chang, Y. T., Lu, M. H., Huang, T. F., Chong, K. Y., Liao, H. R., Cheng, J. C., & Tseng, C. P. (2015). Identification of a novel platelet antagonist that binds to CLEC-2 and suppresses podoplanin-induced platelet aggregation and cancer metastasis. *Oncotarget*, *6*(40), 42733–42748.

Curtis, M. J., Alexander, S. P. H., Cirino, G., George, C. H., Kendall, D. A., Insel, P. A., Izzo, A. A., Ji, Y., Panettieri, R. A., Patel, H. H., Sobey, C. G., Stanford, S. C., Stanley, P., Stefanska, B., Stephens, G. J., Teixeira, M. M., Vergnolle, N., & Ahluwalia, A. (2022). Planning experiments: Updated guidance on experimental design and analysis and their reporting III. *British Journal of Pharmacology*, *179*(15), 3907–3913. https://doi.org/10.1111/bph.15868

Eble, J. A., Beermann, B., Hinz, H. J., & Schmidt-Hederich, A. (2001). $\alpha_2\beta_1$ integrin is not recognized by rhodocytin but is the specific, high affinity target of rhodocetin, an RGD-independent disintegrin and potent inhibitor of cell adhesion to collagen. *The Journal of Biological Chemistry*, *276*(15), 12274–12284. https://doi.org/10.1074/jbc.M009338200

Fuller, G. L., Williams, J. A., Tomlinson, M. G., Eble, J. A., Hanna, S. L., Pohlmann, S., Suzuki-Inoue, K., Ozaki, Y., Watson, S. P., & Pearce, A. C. (2007). The C-type lectin receptors CLEC-2 and Dectin-1, but not DC-SIGN, signal via a novel YXXL-dependent signaling cascade. *The Journal of Biological Chemistry*, *282*(17), 12397–12409. https://doi.org/10.1074/jbc.M609558200

Gitz, E., Pollitt, A. Y., Gitz-Francois, J. J., Alshehri, O., Mori, J., Montague, S., Nash, G. B., Douglas, M. R., Gardiner, E. E., Andrews, R. K., Buckley, C. D., & Watson, S. P. (2014). CLEC-2 expression is maintained on activated platelets and on platelet microparticles. *Blood*, *124*(14), 2262–2270. https://doi.org/10.1182/blood-2014-05-572818

Haining, E. J., Lowe, K. L., Wichaiyo, S., Kataru, R. P., Nagy, Z., Kavanagh, D. P., Lax, S., Di, Y., Nieswandt, B., Ho-Tin-Noé, B., Mehrara, B. J., & Watson, S. P. (2021). Lymphatic blood filling in CLEC-2-deficient mouse models. *Platelets*, *32*(3), 352–367. https://doi.org/10.1080/09537104.2020.1734784

Izquierdo, I., Barrachina, M. N., Hermida-Nogueira, L., Casas, V., Morán, L. A., Lacerenza, S., Pinto-Llorente, R., Eble, J. A., Ríos, V. D., Domínguez Medina, E., & García, A. (2020). A comprehensive tyrosine phosphoproteomic analysis reveals novel components of the platelet CLEC-2 signaling cascade. *Thrombosis and Haemostasis*, *120*(2), 262–276. https://doi.org/10.1055/s-0039-3400295

Kempster, C., Butler, G., Kuznecova, E., Taylor, K. A., Kriek, N., Little, G., Sowa, M. A., Sage, T., Johnson, L. J., Gibbins, J. M., & Pollitt, A. Y. (2022). Fully automated platelet differential interference contrast image analysis via deep learning. *Scientific Reports*, *12*(1), 4614. https://doi.org/10.1038/s41598-022-08613-2

Lim, S. E., Joseph, M. D., de Winde, C. M., Acton, S. E., & Simoncelli, S. (2023). Quantitative single molecule analysis of podoplanin clustering in fibroblastic reticular cells uncovers CD44 function. *Open Biology*, *13*(5), 220377. https://doi.org/10.1098/rsob.220377

Lipinski, C. A., Lombardo, F., Dominy, B. W., & Feeney, P. J. (2001). Experimental and computational approaches to estimate solubility and permeability in drug discovery and development settings. *Advanced Drug Delivery Reviews*, *46*(1–3), 3–26. https://doi.org/10.1016/s0169-409x(00)00129-0

Ma, Y. Q., Qin, J., & Plow, E. F. (2007). Platelet integrin $\alpha_{IIb}\beta_3$: Activation mechanisms. *Journal of Thrombosis and Haemostasis*, *5*(7), 1345–1352. https://doi.org/10.1111/j.1538-7836.2007.02537.x

Meng, D., Luo, M., & Liu, B. (2021). The role of CLEC-2 and its ligands in thromboinflammation. *Frontiers in Immunology*, *12*, 688643. https://doi.org/10.3389/fimmu.2021.688643

Morán, L. A., Di, Y., Sowa, M. A., Hermida-Nogueira, L., Barrachina, M. N., Martin, E., Clark, J. C., Mize, T. H., Eble, J. A., Moreira, D., Pollitt, A. Y., & García, Á. (2022). Katacine is a new ligand of CLEC-2 that acts as a platelet agonist. *Thrombosis and Haemostasis*, *122*(8), 1361–1368. https://doi.org/10.1055/a-1772-1069

Nagae, M., Morita-Matsumoto, K., Kato, M., Kaneko, M. K., Kato, Y., & Yamaguchi, Y. (2014). A platform of C-type lectin-like receptor CLEC-2 for binding O-glycosylated podoplanin and nonglycosylated

rhodocytin. *Structure*, *22*(12), 1711–1721. https://doi.org/10.1016/j.str.2014.09.009

Nakamura-Ishizu, A., Takubo, K., Kobayashi, H., Suzuki-Inoue, K., & Suda, T. (2015). CLEC-2 in megakaryocytes is critical for maintenance of hematopoietic stem cells in the bone marrow. *The Journal of Experimental Medicine*, *212*(12), 2133–2146. https://doi.org/10.1084/jem.20150057

NCBI. (2024a). PubChem bioassay record for AID 1259372, Source: The Scripps Research Institute Molecular Screening Center.

NCBI. (2024b). PubChem bioassay record for bioactivity AID 1259310 - SID 333203465, Source: The Scripps Research Institute Molecular Screening Center.

Peppard, J., Glickman, F., He, Y., Hu, S. I., Doughty, J., & Goldberg, R. (2003). Development of a high-throughput screening assay for inhibitors of aggrecan cleavage using luminescent oxygen channeling (AlphaScreen). *Journal of Biomolecular Screening*, *8*(2), 149–156. https://doi.org/10.1177/1087057103252308

Pollitt, A. Y., Grygielska, B., Leblond, B., Desire, L., Eble, J. A., & Watson, S. P. (2010). Phosphorylation of CLEC-2 is dependent on lipid rafts, actin polymerization, secondary mediators, and Rac. *Blood*, *115*(14), 2938–2946. https://doi.org/10.1182/blood-2009-12-257212

Pollitt, A. Y., Poulter, N. S., Gitz, E., Navarro-Nunez, L., Wang, Y. J., Hughes, C. E., Thomas, S. G., Nieswandt, B., Douglas, M. R., Owen, D. M., Jackson, D. G., & Watson, S. P. (2014). Syk and Src family kinases regulate C-type lectin receptor 2 (CLEC-2)-mediated clustering of podoplanin and platelet adhesion to lymphatic endothelial cells. *The Journal of Biological Chemistry*, *289*(52), 35695–35710. https://doi.org/10.1074/jbc.M114.584284

Severin, S., Pollitt, A. Y., Navarro-Nunez, L., Nash, C. A., Mourao-Sa, D., Eble, J. A., Senis, Y. A., & Watson, S. P. (2011). Syk-dependent phosphorylation of CLEC-2: A novel mechanism of hem-immunoreceptor tyrosine-based activation motif signaling. *The Journal of Biological Chemistry*, *286*(6), 4107–4116. https://doi.org/10.1074/jbc.M110.167502

Spalton, J. C., Mori, J., Pollitt, A. Y., Hughes, C. E., Eble, J. A., & Watson, S. P. (2009). The novel Syk inhibitor R406 reveals mechanistic differences in the initiation of GPVI and CLEC-2 signaling in platelets. *Journal of Thrombosis and Haemostasis*, *7*(7), 1192–1199. https://doi.org/10.1111/j.1538-7836.2009.03451.x

Suzuki-Inoue, K. (2019). Platelets and cancer-associated thrombosis: Focusing on the platelet activation receptor CLEC-2 and podoplanin. *Blood*, *134*(22), 1912–1918. https://doi.org/10.1182/blood.2019001388

Suzuki-Inoue, K., Inoue, O., & Ozaki, Y. (2011). Novel platelet activation receptor CLEC-2: From discovery to prospects. *Journal of Thrombosis and Haemostasis*, *9*(Suppl 1), 44–55. https://doi.org/10.1111/j.1538-7836.2011.04335.x

Tsukiji, N., Osada, M., Sasaki, T., Shirai, T., Satoh, K., Inoue, O., Umetani, N., Mochizuki, C., Saito, T., Kojima, S., Shinmori, H., & Suzuki-Inoue, K. (2018). Cobalt hematoporphyrin inhibits CLEC-2-podoplanin interaction, tumor metastasis, and arterial/venous thrombosis in mice. *Blood Advances*, *2*(17), 2214–2225. https://doi.org/10.1182/bloodadvances.2018016261

Tsukiji, N., & Suzuki-Inoue, K. A.-O. (2023). Impact of Hemostasis on the Lymphatic System in Development and Disease. (1524-4636 (Electronic)).

Watanabe, N., Shinozaki, Y., Ogiwara, S., Miyagasako, R., Sasaki, A., Kato, J., Suzuki, Y., Fukunishi, N., Okada, Y., Saito, T., Iida, Y., & Inokuchi, S. (2024). Diphenyl-tetrazol-propanamide derivatives act as dual-specific antagonists of platelet CLEC-2 and glycoprotein VI. *Thrombosis and Haemostasis*, *124*(3), 203–222. https://doi.org/10.1055/a-2211-5202

Watson, A. A., Brown, J., Harlos, K., Eble, J. A., Walter, T. S., & O'Callaghan, C. A. (2007). The crystal structure and mutational binding analysis of the extracellular domain of the platelet-activating receptor CLEC-2. *The Journal of Biological Chemistry*, *282*(5), 3165–3172. https://doi.org/10.1074/jbc.M610383200

Zhu, T., Cao, S., Su, P. C., Patel, R., Shah, D., Chokshi, H. B., Szukala, R., Johnson, M. E., & Hevener, K. E. (2013). Hit identification and optimization in virtual screening: Practical recommendations based on a critical literature analysis. *Journal of Medicinal Chemistry*, *56*(17), 6560–6572. https://doi.org/10.1021/jm301916b

SUPPORTING INFORMATION

Additional supporting information can be found online in the Supporting Information section at the end of this article.

How to cite this article: Sowa, M. A., Wu, Y., van Groningen, J., Di, Y., van den Hurk, H., Eble, J. A., Gibbins, J. M., García, Á., & Pollitt, A. Y. (2025). High-throughput screen identifies MAS9 as a novel inhibitor of the C-type lectin receptor-2 (CLEC-2)–podoplanin interaction. *British Journal of Pharmacology*, 1–14. https://doi.org/10.1111/bph.70036